The International Archives of the Photogrammetry, Remote Sensing and Spatial Information Sciences, Volume L-4/W1-2026
Free and Open Source Software for Geospatial (FOSS4G) 2026 – Academic Track "Bridging Geospatial Technology and Humanity",
30 August–5 September 2026, Hiroshima, Japan

From Raw ADS-B Signals to Reproducible Flight Trajectories: An Open Geospatial Workflow for Narita International Airport

Junta Tagusari[1,2], Kotarou Kayanuma[2], Junnosuke Umetani[2]

[1] School of Data Science, Yokohama City University, Yokohama, Japan - tagusari.jun.mc@yokohama-cu.ac.jp
[2] Faculty of Engineering, Hokkaido University, Sapporo, Japan - j.tagusari@eng.hokudai.ac.jp

Keywords: ADS-B, flight trajectory, reproducible workflow, open-source geospatial, airport operations, uncertainty.

Abstract

High-resolution flight trajectory data are essential for analysing airport operations, environmental impacts, and aviation safety, yet publicly available aviation statistics typically provide only aggregated indicators such as annual movement counts. This study presents a reproducible open workflow that converts raw ADS-B (Automatic Dependent Surveillance-Broadcast) reception data into analysis-ready flight trajectory datasets while explicitly examining uncertainties introduced throughout the processing pipeline. The workflow is implemented using low-cost open hardware and open-source analytical tools, including an RTL-SDR receiver, a Raspberry Pi single-board computer, and the R programming language. The approach is demonstrated using a full-year dataset collected near Narita International Airport (1 April 2024 to 31 March 2025), yielding 244,105 reconstructed arrival and departure trajectories broadly consistent with published annual movement statistics. The workflow covers temporal normalisation, spatial filtering, coordinate transformation, pressure altitude correction using meteorological observations, trajectory segmentation, runway classification, and quality control. By explicitly documenting each processing step and characterising residual uncertainties, the study provides a transparent and transferable foundation for aviation-related geospatial research and establishes a basis for data reuse in environmental assessment, urban planning, and open public information provision.

1. Introduction

Detailed flight trajectory data play a foundational role across a wide range of policy and operational domains. Building numerical models of aircraft noise exposure to monitor and mitigate community impacts requires accurate spatial and temporal information on aircraft movements (World Health Organization Regional Office for Europe, 2018, Feng et al., 2023). Urban and transport planning require an understanding of how airspace is used in the vicinity of airports, particularly in relation to residential areas. Transparent public communication about aviation activity is increasingly demanded by communities located beneath flight paths, and safety analysis depends on the availability of high-resolution positional records capable of revealing deviations from standard approach and departure procedures.

Despite this demand, official aviation statistics are predominantly aggregated: annual movement counts and published schedules convey the volume of operations but do not preserve the three-dimensional trajectories required for spatial analysis at fine scales. Aircraft positional information is collected systematically by air traffic control authorities, but access to such data is typically restricted for operational and regulatory reasons and is not generally available to independent researchers or local governments.

Commercial flight-tracking services such as Flightradar24 and FlightAware aggregate ADS-B (Automatic Dependent Surveillance-Broadcast) signals from a global network of volunteer receivers and present the resulting trajectories through web interfaces and licensed data products. The OpenSky Network, a community-operated global ADS-B sensor network, has also been established specifically to support research (Schäfer et al., 2014). While these platforms are technically capable and widely used, they impose licensing restrictions that limit reproducibility and redistribution, and their analytical workflows are proprietary and unavailable for independent inspection or adaptation.

ADS-B is a surveillance technology through which aircraft periodically broadcast messages encoding their position, altitude, velocity, and identification using GNSS-derived measurements. The ICAO (International Civil Aviation Organization) standardises the technical specifications of ADS-B (International Civil Aviation Organization, 2007), and its use has been mandated for equipped aircraft in controlled airspace across major jurisdictions. The 1090 MHz frequency band used by the ADS-B system is accessible with commodity software-defined radio hardware at a cost of a few tens of US dollars, enabling independent reception of aircraft signals without any proprietary infrastructure. Open-source decoding software (FlightAware, 2014) allows these signals to be converted into structured positional records suitable for further processing. This accessibility has prompted a growing body of research exploiting ADS-B for purposes ranging from airspace analysis and trajectory modelling to aviation security and emissions estimation (Olive and Basora, 2020).

However, the literature describing end-to-end workflows for converting raw ADS-B reception data into curated geospatial datasets suitable for policy-relevant analysis remains limited. Studies that use ADS-B data often obtain it from existing aggregators such as the OpenSky Network rather than operating independent reception infrastructure, and many analytical pipelines are described only partially or are not released as reproducible implementations.

This study addresses these gaps by presenting and evaluating a complete, reproducible workflow implemented in the R programming language that processes raw ADS-B reception data through all stages from decoding to curated trajectory delivery. The workflow and associated processing scripts are released as an open-source R repository accompanying this paper (Tagusari, 2026). Its design prioritises transparency, transferability, and explicit uncertainty documentation, enabling replication at other airports without modification to core logic. The study uses Narita International Airport in Japan as a demonstration environment, both because of its operational complexity and scale, and because it represents a case where locally operated open infrastructure can produce a dataset complementary to what global commercial platforms offer. Aircraft noise has been a sustained community concern in the area surrounding the airport, and planned infrastructure expansions — including runway extension and new runway construction scheduled for completion by 2029 — create particular impetus for persistent, locally archived trajectory data capable of documenting changes in flight path distributions over time.

2. Methods

2.1 Reception Infrastructure and Data Collection

ADS-B signals broadcast on the 1090 MHz frequency were received using a purpose-built, low-cost hardware configuration. The receiving system consists of a 1090 MHz bandpass antenna, an RTL-SDR USB receiver, and a Raspberry Pi 4B single-board computer. The receiver was installed at a site in the vicinity of Narita International Airport. Though the distance from the receiver to the runway threshold is approximately 6.5 km and aircraft on the ground cannot be seen from the site, the site is just below the principal approach and departure corridors and provides an unobstructed line to aircraft even at low altitudes during approach and departure.

Received signals were decoded in real time using dump1090-fa (FlightAware, 2014), an open-source ADS-B decoder that interprets Mode S Extended Squitter messages and writes structured output containing, for each received message: a Mode S hexadecimal aircraft identifier (also known as the ICAO 24-bit address), latitude and longitude, atmospheric pressure altitude, ground speed, track angle, vertical rate, and call sign where available.

The dataset used in this study covers the period from 1 April 2024 to 31 March 2025, constituting a complete operational year. Records were written at regular intervals to local storage as tab-delimited text files. Each daily file was then converted to compressed parquet format.

Narita International Airport is a major hub serving both domestic and international routes, with published annual movement statistics of 245,529 commercial movements during the observation period (Narita International Airport Corporation, 2026). Flights operate except during a nighttime curfew from 23:00 to 06:00 local time, and the airport has two parallel runways with distinct operational patterns for arrivals and departures (see Figure 1).

2.2 Data Preprocessing

All processing stages were implemented in R (version 4.5.2) (R Core Team, 2025) using the dplyr package (version 1.1.4) (Wickham et al., 2023) for data manipulation and the sf package (version 1.0.21) (Pebesma, 2018) for spatial operations. Documentation of each processing stage and the characterisation of

Figure 1. Flight pattern examples (white lines) and the spatial filter bounding box (yellow box) around Narita International Airport. The background map is from Geospatial Information Authority of Japan.

uncertainties at each step are provided in the accompanying repository (Tagusari, 2026).

The initial preprocessing stage reads the daily archived files, parses the timestamp fields into a unified POSIX datetime format, and concatenates the records into a single time-ordered dataset. Records lacking valid latitude and longitude values are removed, as are records whose atmospheric pressure altitude field indicates a missing or anomalous value. The resulting dataset is filtered spatially to retain only records falling within a bounding box corresponding to the airspace surrounding Narita International Airport (see Figure 1). Horizontal coordinates are transformed from geographic coordinates (WGS84) into a projected coordinate system using the Japan Plane Rectangular Coordinate System zone IX, which is appropriate to the study area, enabling metric distance calculations in subsequent geometric operations. Atmospheric pressure altitude values reported in feet are converted to metres.

2.3 Altitude Correction

The atmospheric pressure altitude, reported in the ADS-B messages, represents altitude above sea level based on the standard atmosphere model, which assumes a fixed sea-level pressure of 1013.25 hPa (International Civil Aviation Organization, 1993). However, actual surface pressure can deviate from this standard value due to weather conditions, leading to discrepancies between the reported atmospheric pressure altitude and the true geometric altitude above mean sea level.

To correct for this discrepancy, surface pressure observations at a measurement station in Chiba City, which is spatially representative of the Narita International Airport area, were obtained from the Japan Meteorological Agency (Japan Meteorological Agency, 2026). For each ADS-B record, the pressure altitude was corrected to an approximate geometric altitude using the following pressure-altitude relationship inverted with the observed surface pressure:

$$h = h_p - 8.23 \cdot (1013.25 - p)$$

where h is the corrected altitude (m), h_p is the pressure altitude (m), p is the observed surface pressure (hPa).

Note that the absolute altitude at the Narita International Airport is approximately 40 m above mean sea level, so the corrected altitude values from which 40 m is subtracted yield altitude above the airport reference plane.

2.4 Aircraft Attribute Integration

To support fleet-level analysis and facilitate cross-referencing with published movement data, aircraft attribute information was integrated using the OpenSky Network aircraft database. The Mode S hexadecimal identifier present in each ADS-B record was used as a join key to retrieve, where available, the ICAO aircraft type designator, manufacturer name, aircraft registration, and nationality of registration. Aircraft type was encoded using the ICAO type designator to enable grouping by broad fleet categories. In addition, trajectories associated with helicopters and light propeller-driven aircraft were excluded from the dataset as these aircraft types are not expected to follow standard approach and departure paths.

2.5 Trajectory Segmentation

Individual flights were reconstructed from the sequence of positional records by grouping consecutive records sharing the same Mode S identifier. A new trajectory segment was initiated whenever the interval between successive messages from the same aircraft exceeded 600 seconds. This threshold was selected as a conservative criterion for identifying temporal discontinuities likely to reflect either a genuine gap between distinct flights or a reception outage exceeding the typical message broadcast interval.

Each candidate trajectory was then classified as an arrival, departure, or flyover using the first and last points of the trajectory. Where both points are located more than 4 km away from the runway, the trajectory is classified as flyover and excluded from further analysis. Then, the altitude of the two points is compared to infer the flight type: if the trajectory terminates at a lower altitude than its origin, it is classified as an arrival; if it terminates at a higher altitude, it is classified as a departure.

To estimate the runway used for each trajectory and to classify the flight direction, the portion of each trajectory at altitudes above 200 m (low-cut trajectory) was analysed. This threshold excludes ground-level records and focuses the analysis on the airborne portion of the trajectory, where aircraft are most likely following standard approach or departure paths. The perpendicular distance from the lowest-altitude point of each low-cut trajectory to the extended centreline of each runway was calculated, and the runway with the minimum distance was assigned as the runway used for that trajectory. The flight direction (northbound or southbound) was inferred based on the projected position of the first (for departures) and last (for arrivals) points of the low-cut trajectory relative to the runway centreline. The assigned runway, combined with the inferred flight direction (northbound or southbound) and movement type (arrival or departure), yields a classification into eight operational categories reflecting the principal traffic patterns at Narita International Airport (see Figure 1).

As the final step in trajectory reconstruction, fragmented portions of trajectories caused by wide turns moving in and out of the spatial filter were removed. This was done by identifying segments of trajectories that exhibited large time gaps (¿60 seconds) between consecutive records at altitudes above 1000 m.

2.6 Quality Control

A final quality-control stage applied two filters. First, trajectories whose low-cut versions (low-cut trajectories) had fewer than 10 positional records were excluded as insufficiently sampled for reliable geometric characterisation. Second, trajectories with perpendicular distances exceeding 250 m from the lowest point of the low-cut trajectory to the runway centreline were removed.

3. Results

3.1 Overall Trajectory Yield

The number of trajectories initially reconstructed from the raw data was 245,205. Of these, 591 trajectories from helicopters and light propeller-driven aircraft were excluded; a further 303 trajectories with fewer than 10 positional records above 200 m altitude were also removed. In addition, 206 trajectories that exhibited a large distance (>250 m) from the runway centreline at low altitudes were removed. These included trajectories associated with one aircraft that consistently showed large deviations, and 21 additional trajectories from other aircraft. Finally, 244,105 trajectories were retained after quality control.

Published annual aircraft movement statistics for Narita International Airport report 245,529 commercial movements during the observation year (Narita International Airport Corporation, 2026), indicating that the reception and processing pipeline captures real operations at a scale broadly consistent with the known population of movements.

3.2 Fleet Composition

Table **??** shows the distribution of reconstructed trajectories by ICAO aircraft class designator, which encodes the airframe type, engine count, and engine type. The most common class designator is L2J, which corresponds to landplane aircraft with two jet engines, consistent with the prevalence of narrow-body commercial airliners in the traffic mix at Narita International

ICAO Class Designator	Count
L2J (aircraft with 2 jet engines)	200,647
L4J (aircraft with 4 jet engines)	13,491
L3J (aircraft with 3 jet engines)	591
L2T (aircraft with 2 turboprop engines)	28
A5 (regional jets)	28
L1T (light single-engine aircraft)	6
L1P (light piston-engine aircraft)	4
Not reported	29,310

Table 1. Aircraft class composition

ICAO Type Designator	MTOW (t)	Count
A320 (Airbus A320)	75	36,551
B738 (Boeing 737-800)	78.2	32,059
B788 (Boeing 787-8)	227	21,051
B789 (Boeing 787-9)	245	20,450
A321 (Airbus A321)	89	17,839
A21N (Airbus A321neo)	97	15,333
A20N (Airbus A320neo)	79	14,863
B763 (Boeing 767-300)	175.5	14,212
A333 (Airbus A330-300)	212	11,457
B77W (Boeing 777-300ER)	351	9,187

Table 2. Top ten most frequently observed ICAO aircraft type designators, with the MTOW (Maximum Takeoff Weight) in metric tons and the count of trajectories associated with each type.

Airport. The presence of L4J and L3J classes, which correspond to larger wide-body jets, reflects the airport's role as an international hub serving long-haul routes. The small numbers of trajectories in the remaining categories (L2T, A5, L1T, and L1P) likely correspond to general aviation and non-commercial operations in the vicinity of the airport. The "Not reported" category consists of trajectories whose ICAO aircraft class designator was absent from the OpenSky Network database; of these 29,310 trajectories, only 703 lacked aircraft information entirely, while the remainder had a known ICAO type designator but no corresponding class designator recorded.

Table **??** lists the top ten most frequently observed ICAO aircraft type designators in the reconstructed dataset. The most common types include the Airbus A320 family (A320, A321, A21N, A20N) and the Boeing 737-800 (B738), which are widely used narrow-body airliners for short- and medium-haul routes. The presence of wide-body types such as the Boeing 787-8 (B788), Boeing 787-9 (B789), Boeing 767-300 (B763), Airbus A330-300 (A333), and Boeing 777-300ER (B77W) reflects the international traffic served by Narita International Airport.

3.3 Flight Type Distribution

Table **??** summarises the distribution of reconstructed trajectories by flight type (arrival or departure), runway (A or B), and direction (northbound or southbound). Runway A (16R/34L), which is longer than Runway B (16L/34R), is predominantly used for departures, while Runway B is predominantly used for arrivals, consistent with published information on operational patterns at Narita International Airport (Narita City, 2025).

Type	Runway	Direction	Count
Departure	A	Northbound	63,766
		Southbound	56,705
	B	Northbound	930
		Southbound	722
Arrival	A	Northbound	11,554
		Southbound	9,900
	B	Northbound	54,014
		Southbound	46,514

Table 3. Summary of reconstructed trajectories by flight type, runway and direction.

Time Interval (Local Time)	Count	Average per day
00:00 - 01:00	46	0.1
01:00 - 02:00	1	0.0
02:00 - 03:00	1	0.0
03:00 - 04:00	0	0.0
04:00 - 05:00	0	0.0
05:00 - 06:00	0	0.0
06:00 - 07:00	8,168	22.4
07:00 - 08:00	10,170	27.9
08:00 - 09:00	10,116	27.7
09:00 - 10:00	13,373	36.6
10:00 - 11:00	11,675	32.0
11:00 - 12:00	15,636	42.8
12:00 - 13:00	15,811	43.3
13:00 - 14:00	15,902	43.6
14:00 - 15:00	17,993	49.3
15:00 - 16:00	19,666	53.9
16:00 - 17:00	16,627	45.6
17:00 - 18:00	18,604	51.0
18:00 - 19:00	19,188	52.6
19:00 - 20:00	16,874	46.2
20:00 - 21:00	13,243	36.3
21:00 - 22:00	10,126	27.7
22:00 - 23:00	8,228	22.5
23:00 - 00:00	2,657	7.3

Table 4. Distribution of reconstructed trajectories by time of day, showing the total number of movements occurring in each 1-hour interval and their average per day.

3.4 Temporal Distribution

Table **??** shows the distribution of reconstructed trajectories by time of day. The temporal distribution of movements exhibits a clear diurnal pattern, with the highest volumes occurring during the daytime and early evening hours, and a pronounced drop during the nighttime curfew period from 23:00 to 06:00 local time. However, a small number of flights were detected during the curfew hours, and the times shown represent departure or arrival moments and may not reflect when the aircraft was overflying residential areas.

3.5 Flight Trajectory Patterns

Figures 2 to 9 show example trajectory patterns. All trajectories lead to or depart from the runways, but the spatial patterns vary by runway and movement type. Trajectories for departures from Runway A in the northbound direction (Figure 2) exhibit numerous turns after taking off from the runway, while aircraft departing from Runway A in the southbound direction (Figure 3) travel straight for a longer distance before reaching the open sea, where they make turns. Arrival paths (Figures 4 and 5) show more consistent patterns, with aircraft following a more direct approach path to the runway. One notable trajectory for an arrival at Runway A (Figure 4) represents an aircraft that initially attempted to land on Runway B before executing a go-around and landing on Runway A. When comparing the same operation type and direction, no clear differences in trajectory patterns were observed between Runway A and Runway B.

Figure 10 shows the vertical cross section of trajectories for arrivals at Runway B in the northbound direction. Although there are some outliers, most trajectories follow a consistent descent

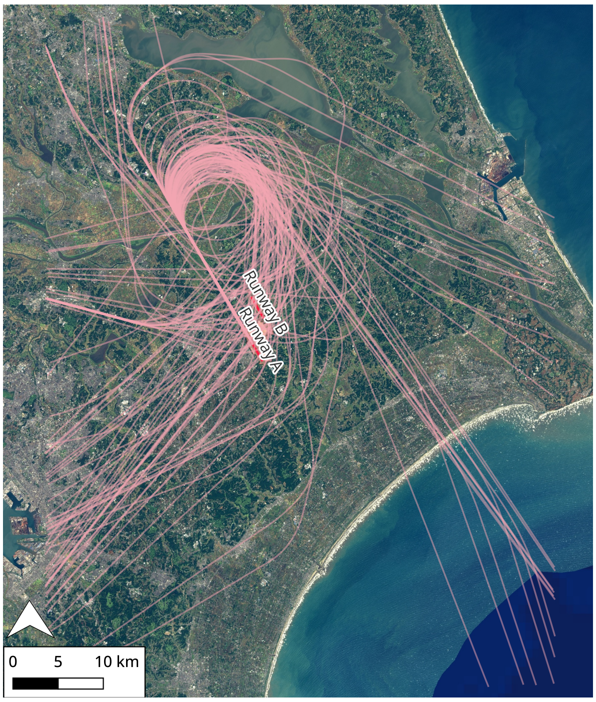

Figure 2. Trajectory example patterns for departures from Runway A in the northbound direction.

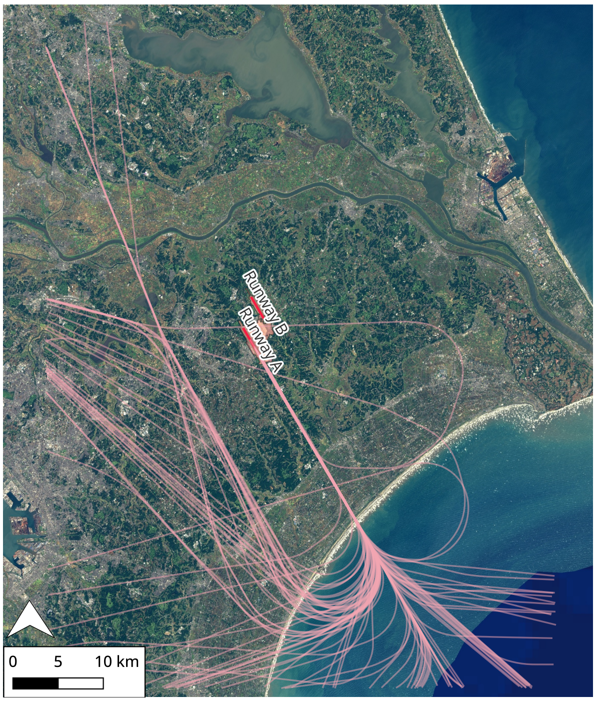

Figure 3. Trajectory example patterns for departures from Runway A in the southbound direction.

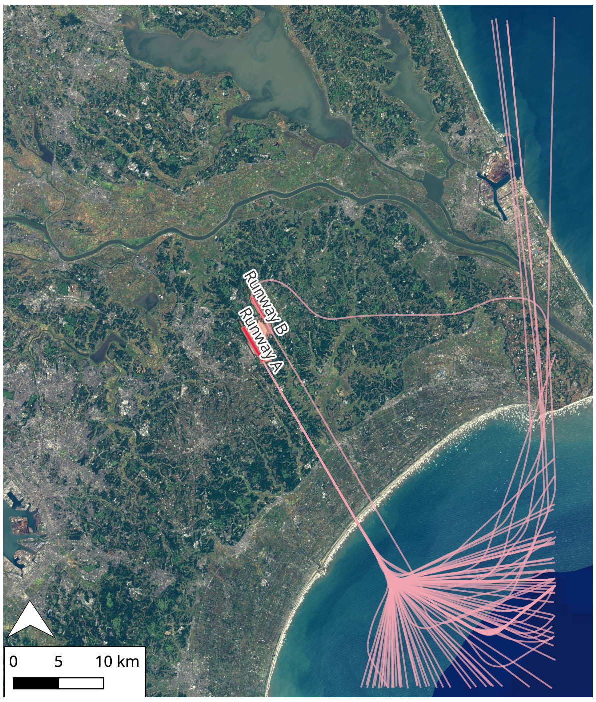

Figure 4. Trajectory example patterns for arrivals at Runway A in the northbound direction.

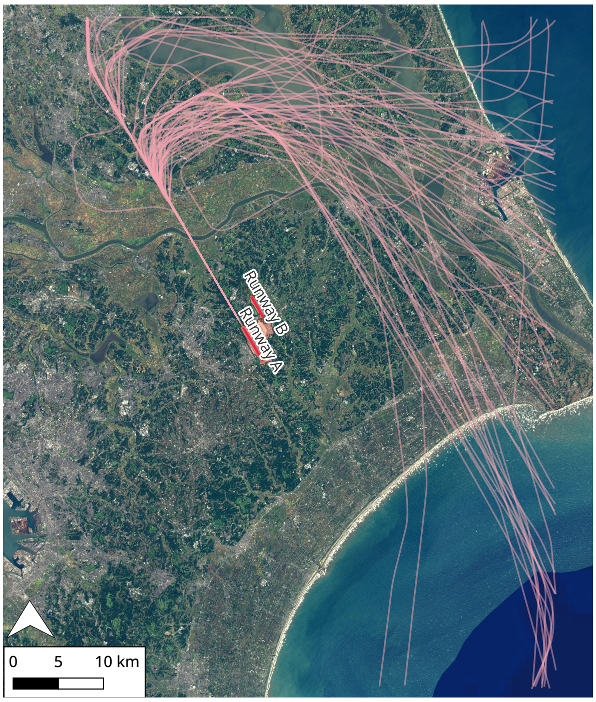

Figure 5. Trajectory example patterns for arrivals at Runway A in the southbound direction.

profile along a 3.1-degree glide slope, close to the standard 3-degree instrument approach angle for commercial aircraft, and terminate at the runway threshold (red circle).

4. Discussion

4.1 Workflow Transferability and the Open-Source Approach

The principal contribution of this study is a transparent, modular, and fully documented workflow that transforms raw ADS-B reception data into a curated geospatial flight trajectory dataset. Each processing stage is implemented as an independent,

Figure 6. Trajectory example patterns for departures from Runway B in the northbound direction.

Figure 7. Trajectory example patterns for departures from Runway B in the southbound direction.

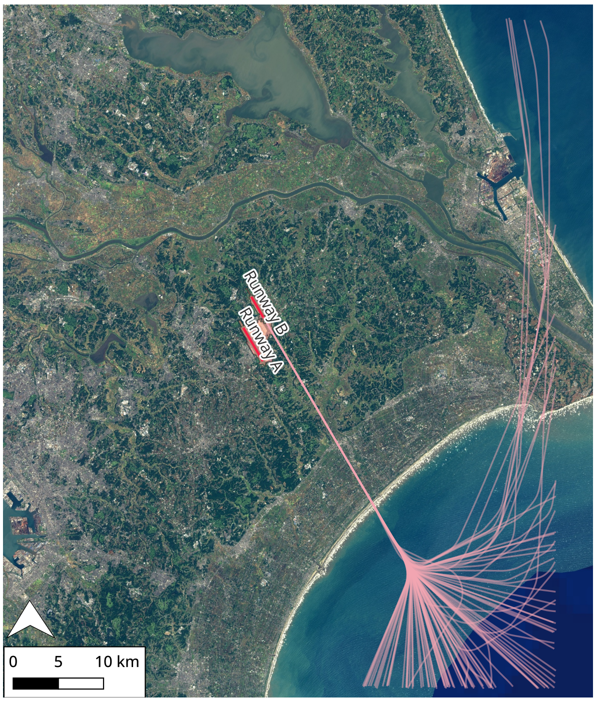

Figure 8. Trajectory example patterns for arrivals at Runway B in the northbound direction.

Figure 9. Trajectory example patterns for arrivals at Runway B in the southbound direction.

inspectable function. The workflow has been released as an open-source repository so that other researchers and practitioners can apply it to different airports, time periods, and analytical objectives without reliance on any proprietary components.

This transferability addresses a gap that commercial flight-tracking platforms are not designed to fill. Services such as Flightradar24 and FlightAware provide excellent global coverage and convenient access to historical data for general use, but they do not expose their processing pipelines, do not offer fine-grained uncertainty documentation, and impose licensing terms that constrain redistribution and derivative research. The present workflow, by contrast, allows practitioners at any airport to establish independent data collection and processing infrastructure using commodity hardware costing less than 100 USD, and to produce trajectory datasets whose provenance and limitations are fully characterised. This transparency is particularly valuable in regulatory and public-engagement contexts

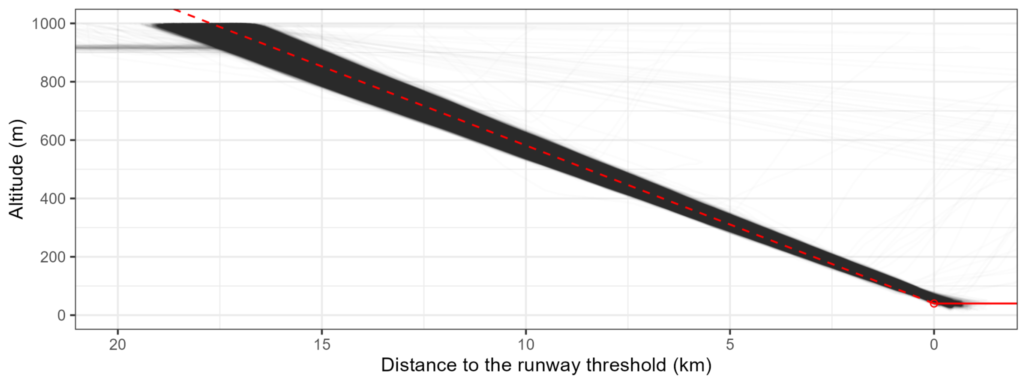

Figure 10. Vertical cross section of trajectory for arrivals at Runway B in the northbound direction. The landing point (red circle) is located at the runway threshold, and most trajectories follow a consistent descent profile, following a 3.1-degree glide slope (red dashed line).

where the basis for environmental or operational conclusions must be open to scrutiny. In addition to aggregate patterns, the workflow captures individual non-standard flight events — such as a go-around manoeuvre identified in the Runway A northbound arrival data (Figure 4) — that are absent from published movement statistics but are relevant for safety monitoring and community impact assessment.

4.2 Differentiation Through Local Context and Data Sovereignty

A locally operated workflow offers capabilities that globally aggregated platforms cannot easily replicate. Because data collection is operated independently and data are stored locally, the dataset can be made available to municipal governments, environmental agencies, and research institutions without licensing barriers. Local operators retain full control over retention policies, update frequency, and data-sharing arrangements.

For the specific case of Narita International Airport, the one-year empirical dataset contains operational patterns — runway usage asymmetries, time-of-day distributions, fleet composition — that are not available from any single published statistical source. This locally specific, high-resolution, open dataset constitutes a resource that regional planners, noise consultants, and community representatives can use in ways that would be difficult or costly using commercial data products. The slight under-count of reconstructed trajectories relative to official annual statistics (244,105 versus 245,529, a difference of approximately 0.6%) is attributable to reception outages and to aircraft that operate without ADS-B transponders; the close agreement provides a useful sanity check on the overall completeness of the pipeline.

4.3 Uncertainty Characterisation

The workflow explicitly documents and where possible quantifies three primary sources of uncertainty. First, ADS-B positional accuracy depends on the quality of the GNSS receiver aboard each aircraft; published characterisations suggest horizontal accuracy on the order of a few tens of metres under normal conditions, though this varies by aircraft type and avionics configuration (Zhang et al., 2011). Altitude accuracy is subject to additional barometric pressure calibration variability on the order of tens of metres under standard conditions (Olive et al., 2024). Second, the altitude correction step introduces uncertainty through the spatial representativeness of the surface pressure observations, which are available only at the Chiba City measurement station and do not capture mesoscale pressure gradients that may cause systematic offsets at particular approach azimuths. Third, reception rate varies with aircraft range, antenna siting, and local radio-frequency environment. Gaps in reception can lead to trajectory segments with reduced spatial resolution, affecting the precision of descent-profile reconstruction and the reliability of runway-assignment classification at low altitudes.

An independent indicator of vertical trajectory quality is provided by the reconstructed descent profiles for Runway B northbound arrivals (Figure 10), where trajectories converge on a best-fit glide slope of 3.1 degrees, consistent with the standard 3-degree instrument approach angle, and terminate at the runway threshold. This geometric consistency supports the conclusion that the altitude reconstruction captures real approach profiles at a resolution sufficient for macro-scale spatial analysis.

These characterisations are intended to support informed use of the dataset. Applications that require high vertical accuracy, such as obstacle-clearance analysis, should be approached with caution pending independent validation. Applications that depend primarily on large-scale temporal and spatial distributions, such as noise exposure mapping and emissions inventory preparation, are less sensitive to residual altitude uncertainty and can proceed on the basis of the quality-control documentation provided.

4.4 Applications and Open Ecosystem Contribution

For airport operational analysis, the dataset enables characterisation of traffic patterns, runway usage distributions, and temporal variability at a resolution not available from published statistics.

For environmental impact assessment, trajectory data constitute a primary input to noise prediction models and flight-path-based emissions calculations. In the specific case of Narita International Airport, aircraft noise has been a long-standing environmental concern for surrounding communities, and quantitative characterisation of flight trajectories is a prerequisite for evidence-based noise impact evaluation. Open, locally produced datasets reduce dependence on commercial data access and enable municipalities and environmental agencies to conduct independent assessments or to verify vendor-supplied analyses, and can be spatially integrated with municipal datasets —

such as residential land-use maps and population distributions — to support targeted noise mitigation planning.

For public transparency, a publicly accessible dataset of aircraft movements in the vicinity of an airport supports community engagement by providing verifiable, independently produced information about operations.

For monitoring the impact of planned infrastructure changes, persistent local data collection offers capabilities that commercial services cannot guarantee. Narita International Airport is scheduled to undergo runway extension and new runway construction by 2029. Continuous archiving of trajectory data before, during, and after these developments will enable quantitative before-and-after comparison of flight path distributions and their spatial footprint over residential areas — a capability that depends on long-term data continuity and cannot be reliably replicated from services subject to retrospective access restrictions.

The open-source release of the workflow, together with documentation of the processing pipeline and uncertainty characterisation, is intended to contribute to the broader FOSS4G community goal of making geospatial analysis transparent and reproducible. The workflow demonstrates how commodity open hardware and open analytical software can be integrated into a complete, reusable spatial data pipeline applicable to a class of infrastructure monitoring problems that extend well beyond aviation.

5. Conclusions

This study has presented a reproducible, open-source R workflow for converting raw ADS-B reception data into curated geospatial flight trajectory datasets, demonstrated through a one-year empirical dataset at Narita International Airport. Application to the Narita dataset produced 244,105 trajectories consistent with published annual movement statistics, with documented residual altitude uncertainty and trajectory-level quality-control exclusions below one per cent. The transparent, modular pipeline with explicit uncertainty characterisation and an open-source implementation addresses a gap in locally operated, open aviation geospatial analysis, and demonstrates how commodity hardware and open analytical software can support reproducible spatial data pipelines applicable to a range of infrastructure monitoring contexts.

Future work will focus on validating the workflow against independent data sources at other airports, developing a standardised output data model to facilitate cross-study comparison and data reuse, and integrating the trajectory dataset with downstream analytical tools for noise modelling and emissions estimation.

References

Feng, H., Zhou, Y., Zeng, W., Ding, C., 2023. Review on Metrics and Prediction Methods of Civil Aviation Noise. *International Journal of Aeronautical and Space Sciences*, 24, 1199–1213.

FlightAware, 2014. Dump1090-fa: FlightAware's dump1090 fork. www.github.com/flightaware/dump1090 (9 June 2026).

International Civil Aviation Organization, 1993. Manual of the ICAO Standard Atmosphere: Extended to 80 Kilometres (262 500 Feet) (Third Edition).

International Civil Aviation Organization, 2007. Aeronautical Telecommunications Volume IV: Surveillance and Collision Avoidance Systems (Fourth Edition).

Japan Meteorological Agency, 2026. Historical weather data. www.data.jma.go.jp/stats/etrn/ (15 June 2026) (in Japanese).

Narita City, 2025. Fiscal year 2024 aircraft noise report. www.city.narita.chiba.jp/environment/page0116_00006.html (15 June 2026) (in Japanese).

Narita International Airport Corporation, 2026. Traffic Statistics. www.narita-airport.jp/en/company/airport-operation/operation/ (15 June 2026).

Olive, X., Basora, L., 2020. Detection and Identification of Significant Events in Historical Aircraft Trajectory Data. *Transportation Research Part C: Emerging Technologies*, 119, 102737.

Olive, X., Krummen, J., Figuet, B., Alligier, R., 2024. Filtering Techniques for ADS-B Trajectory Preprocessing. *Journal of Open Aviation Science*, 2(2).

Pebesma, E., 2018. Simple Features for R: Standardized Support for Spatial Vector Data. 10, 439.

R Core Team, 2025. R: A language and environment for statistical computing. www.r-project.org/ (9 June 2026).

Schäfer, M., Strohmeier, M., Lenders, V., Martinovic, I., Wilhelm, M., 2014. Bringing up OpenSky: A large-scale ADS-B sensor network for research. *IPSN-14 Proceedings of the 13th International Symposium on Information Processing in Sensor Networks*, 83–94.

Tagusari, J., 2026. adsb-to-trajectories-narita. www.gitlab.com/jtagusari/adsb-to-trajectories-narita (15 June 2026).

Wickham, H., François, R., Henry, L., Müller, K., Vaughan, D., 2023. dplyr: A grammar of data manipulation. www.cran.r-project.org/package=dplyr (15 June 2026). R package version 1.1.4.

World Health Organization Regional Office for Europe, 2018. *Environmental Noise Guidelines for the European Region*. World Health Organization Regional Office for Europe.

Zhang, J., Liu, W., Zhu, Y., 2011. Study of ADS-B Data Evaluation. *Chinese Journal of Aeronautics*, 24, 461–466.